

IDENTIFICATION OF QPO FREQUENCY OF GRS 1915+105 AS THE RELATIVISTIC DYNAMIC
FREQUENCY OF A TRUNCATED ACCRETION DISKRANJEEV MISRA¹, DIVYA RAWAT^{*2}, J S YADAV², PANKAJ JAIN²Inter-University Center for Astronomy and Astrophysics, Ganeshkhind, Pune 411007, India and
Department of physics, IIT Kanpur, Kanpur, Uttar Pradesh 208016, India

Draft version February 18, 2022

ABSTRACT

We have analyzed *AstroSat* observations of the galactic micro-quasar system GRS 1915+105, when the system exhibited C-type Quasi-periodic Oscillations (QPOs) in the frequency range of 3.4-5.4 Hz. The broad band spectra (1-50 keV) obtained from simultaneous LAXPC and SXT can be well described by a dominant relativistic truncated accretion disk along with thermal Comptonization and reflection. We find that while the QPO frequency depends on the inner radii with a large scatter, a much tighter correlation is obtained when both the inner radii and accretion rate of the disk are taken into account. In fact, the frequency varies just as the dynamic frequency (i.e. the inverse of the sound crossing time) as predicted decades ago by the relativistic standard accretion disk theory for a black hole with spin parameter of ~ 0.9 . We show that this identification has been possible due to the simultaneous broad band spectral coverage with temporal information as obtained from *AstroSat*.

Keywords: accretion, accretion disks — black hole physics — X-rays: binaries — X-rays: individual: GRS 1915+105

1. INTRODUCTION

For a test particle orbiting a black hole, there are three characteristic frequencies depending on the radius (Stella et al. 1999a,b). The first is the Keplerian frequency which is the inverse of the time period of the orbit. There is the periastron precession frequency which is the Keplerian frequency minus the Epicyclic one and relates to how an orbit will precess in General Relativity. There is also the Lense-Thirring precession frequency which is related to the wobbling of the orbit out of the plane which arises only in General Relativity when the black hole is spinning.

Apart from these three relativistic test particle frequencies, there are two other frequencies related to the two characteristic speeds in an accretion disk, the sound ($c_s(r)$) and the radial inflow speeds ($v_r(r)$) where r is the radial distance. The dynamical frequency is the inverse of the sound crossing time i.e. $f_{dyn} \sim c_s(r)/r$. In the standard thin relativistic accretion disk (Shakura & Sunyaev 1973; Novikov & Thorne 1973) the sound speed is

$$c_s(r) = h(r)(GM/r^3)^{1/2} A^{-1} B^1 C^{-1/2} D^{1/2} E^{1/2} \quad (1)$$

where M is the mass of the black hole. The relativistic terms A , B , C , D , E are functions of r and the black hole spin parameter, a . They asymptotically tend to unity in the Newtonian limit i.e. when r tends to infinity. The scale height in the inner regions of the disk is given by

$$h(r, a) \sim 10^6 \text{cm} \dot{M}_{18} A^2 B^{-3} C^{1/2} D^{-1} E^{-1} L \quad (2)$$

where \dot{M}_{18} is the accretion rate in units of 10^{18} grams/second. The relativistic term L is a function of r and a and arises due to the relativistic phenomenon of the existence of a last stable orbit at which the disk flow no longer depends on viscosity and the height vanishes.

Thus

$$\frac{f_{dyn}}{\dot{M}_{18}} = N \ 8979 \text{ Hz} (r/r_g)^{-2.5} (M/12.4M_\odot)^{-2} \\ \times A^1 B^{-2} D^{-0.5} E^{-0.5} L \quad (3)$$

where $r_g = GM/c^2$ is the Gravitational radius and the mass of the black hole, M has been scaled by $12.4M_\odot$, which is reported black hole mass for the source GRS 1915+105 (Reid et al. 2014). N is a factor of order unity to incorporate the assumptions made in the standard accretion disk theory especially in the radiative transfer equation. It should be emphasised that A, B, D, E and L are functions of radii and are important for small radii, $r < 10r_g$. Thus the functional form of f_{dyn} significantly deviates from its Newtonian dependence of $\propto r^{-2.5}$ in this regime. Note that f_{dyn} does not depend on the unknown turbulent viscosity parameter α of the standard disk theory in contrast to the viscous time-scale $\tau_{visc} \sim r/v_r$, where v_r is the radial inflow velocity of the disk. τ_{visc} is an order of magnitude higher than the dynamical time-scale and depends inversely on both α and accretion rate squared.

X-ray binaries show variability on a wide range of time-scales which include broad band noise and nearly periodic oscillations termed as Quasi-periodic Oscillations (QPOs) (van der Klis 2005). For systems harbouring black holes, the QPO frequency ranges from milli-Hertz to hundreds of Hertz prompting classification in very low (milli-Hz), low (Hz) and high frequency QPOs (~ 100 Hz). Low frequency QPOs occur at different spectral states and have been further classified as A, B and C type QPOs (Wijnands et al. 1999; Homan et al. 2001; Remillard et al. 2002; Casella et al. 2004). This multitude of QPOs suggested that they perhaps correspond to different characteristic timescales of the system described above. Moreover since the frequency of a particular type of QPO varies, the radius responsible for

the phenomenon should also be varying. An attractive candidate for this radius is the truncation or inner radius of a standard disk beyond which there is a hot inner flow (Shapiro et al. 1976; Narayan & McClintock 2008). Since the characteristic time-scales depend on General Relativistic corrections, identification of a QPO frequency with one, opens the exciting possibility of testing the theory in the strong field regime.

However, as discussed below it has proved to be difficult to make reliable and independent estimate of the inner disk radius. Indirect schemes have been employed to identify the QPO frequencies. For example, taking advantage of the different radial dependencies of the characteristic frequencies, correlation between frequencies of different QPOs or breaks in the broad band noise have been used to identify the QPO frequencies (Psaltis et al. 1999; Belloni et al. 2002; Stella et al. 1999a,b). This method depends on the relatively rare detection of more than two QPOs at the same time (Motta et al. 2014). Another method has been to use the correlation of the QPO frequency with some other features, such as the high energy spectral index, as proxy for a characteristic radius (Titarchuk & Osherovich 1999). However, since the dependence of the high energy spectral index with radius is model dependent and sensitive to assumptions of the unknown viscosity, the best one can obtain are empirical scaling relations, which have proved useful to compare between different black hole systems (Titarchuk & Fiorito 2004).

The inner radius of an accretion disk can be measured by fitting the spectra of these sources with a truncated accretion disk model (Muno et al. 1999; Sobczak et al. 2000). Till recently, the detection of QPOs in black hole systems have been done by the Proportional Counter Array (PCA) on board the Rossi X-ray Timing Experiment (RXTE) observatory. Since the radius has to be measured strictly simultaneously with the QPO, the spectral analysis needed to be restricted to data obtained from RXTE. However, the PCA had a relatively poor spectral resolution and its effective energy range was from 3 to 20 keV, while the typical maximum colour temperature of the disk is around 1 keV. Moreover, since the spectral data was restricted in the energy range, simple models had to be used to fit the spectra. This limited energy range led to severe systematic uncertainties in the inner disk radius with some values being unphysically small. Moreover, the results were sometimes contradictory like QPO frequency increasing with radius for one system while decreasing for another (Sobczak et al. 2000). Nevertheless, correlations have been observed between the frequency and the radius which have been used as evidence for some models, although there were large scatter in the estimated values (Mikles et al. 2009). A critical limitation of these earlier works was that these analysis were not sensitive enough to test the variation of the QPO frequency with accretion rate, since that requires broadband data.

The Large Area X-ray Proportional Counter (LAXPC) (Yadav et al. 2016; Agrawal et al. 2017) and the Soft X-ray Telescope (SXT) (Singh et al. 2016, 2017) on board the Indian Space Observatory AstroSat (Agrawal 2017) is ideally suited to study correlation between the QPO frequency and the disc inner radius. The high time precision and the large area of LAXPC provide timing and

spectral information in the 4 - 50 keV band, the SXT provides simultaneous spectral coverage in the low 1.0 - 5.0 keV band. As reported by Rawat et al. (2019), AstroSat observed the black hole system GRS 1915+105 from 28th March 2017 18:03:19 till 29th March 2017 19:54:07 when the source transited from a relatively steady state called χ class, through an intermediate state (IMS), to a flaring state (heartbeat state(HS)) where large amplitude oscillations are seen. All through the observation, the source exhibited C-type QPOs in the frequency range 3.4-5.4 Hz.

In this work, we examine the spectral evolution of the source during this observation and supplement the results with observations made two days later on 1st April 2017, when the source shows both χ and 'heartbeat state' with QPOs in the same frequency range. It was fortuitous that the source was undergoing a transition and showed a QPO all through enabling us to study the spectral properties of the source and correlate them with the varying QPO frequency.

2. DATA ANALYSIS

2.1. Timing Analysis

Rawat et al. (2019) split the 28th March 2017 observation into several segments and presented the timing properties for each of them. From the Power Density Spectra (PDS) they obtained the QPO frequencies for segments corresponding to the χ , intermediate and heartbeat states. Following Rawat et al. (2019) we do the same analysis for the *AstroSat* LAXPC observation of GRS 1915+105 during 1st April 2017 00:03:21 till 1st April 14:38:01. The data was analyzed for the two units LAXPC 10 and LAXPC 20, using the *LaxpcSoft*¹. Like the earlier observation, the source exhibited χ and heartbeat states which were divided into 6 segments (2 for χ and 4 for the heartbeat state). Lightcurves for representative segments for a χ and heartbeat state are shown in top panel of Figure 1 and the corresponding PDS are shown in the bottom panel. The PDS were fitted using lorentzian functions and the QPO frequency with error was estimated using the same technique given in Rawat et al. (2019). Thus combining the two observations we have a total of 16 segments (5 for χ , 3 for intermediate and 8 for the heartbeat states) for which the QPO frequency has been estimated and tabulated in the first column of Table 1.

2.2. Spectral Analysis

For each of the 16 segments, simultaneous spectral data was obtained from LAXPC 10, 20 and SXT. The LAXPC spectra, background and response files were generated using the *LaxpcSoft*¹. For SXT data reduction *arf* and *rmf* files are used, details of which are given at *AstroSat* website². The SXT spectra were extracted from a source region of 12 arcmins and the standard background spectra were used for all spectra.

The SXT (energy range 1.0 - 5.0 keV) and LAXPC 10 and 20 (energy range 4 - 50 keV) spectra of each data set was analyzed together using the X-ray spectra fitting software XSPEC (Arnaud 1996) using its inbuilt models. During the spectral fitting gain variation for SXT

¹ <http://astrosat-ssc.iucaa.in/?q=laxpcData>

² <http://astrosat-ssc.iucaa.in/?q=sxtData>

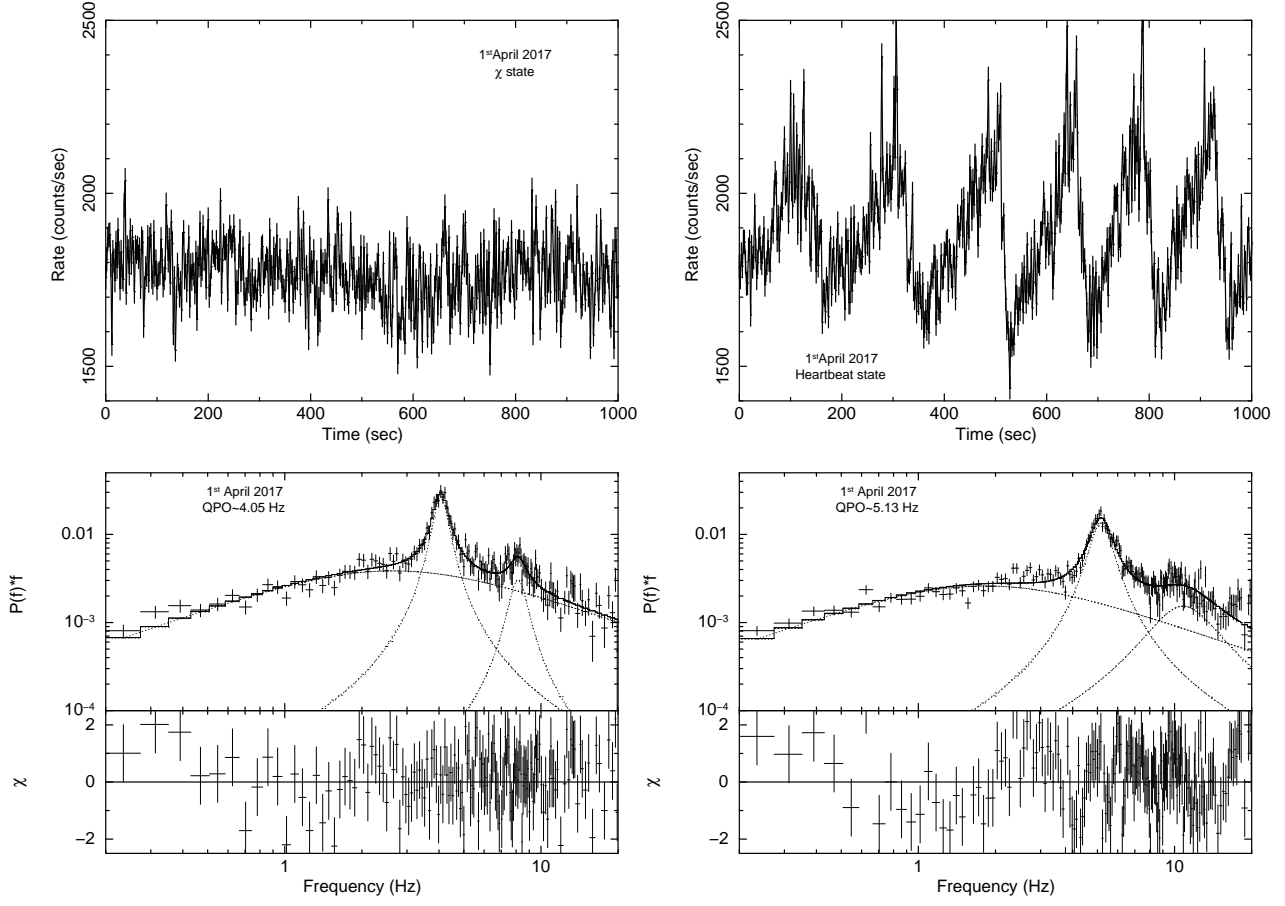


Figure 1. Top panel shows the 2.0 sec binned 1000 sec lightcurves of χ class and heartbeat state. The corresponding PDS in 0.2-20.0 Hz range are shown in bottom panels. LAXPC10 & LAXPC20 are used for lightcurve and PDS extraction here.

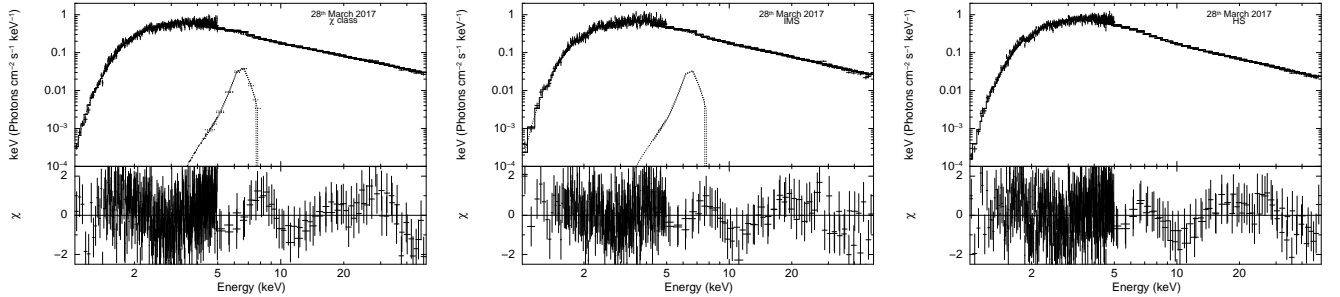


Figure 2. Spectral fitting including residuals are shown for χ state, Intermediate state and heartbeat state.

was taken into account by using the gain fit command in XSPEC. The offset value obtained ranged from 1.4 to 2.4 eV. Additional systematic error of 3% was included. To take into account possible uncertainties in the effective area of the instruments a variable constant was included to the LAXPC 10 and 20 spectra relative to SXT, whose values ranged from 0.81 to 0.92.

The spectra were fitted using the relativistic disk model, “kerrd” (Ebisawa et al. 2003), and the convolution model “simpl” (Steiner et al. 2009) to take into account the Comptonization of the disk photons in the inner flow. The accretion rate and the inner radius of the disk were estimated from the best fit values obtained from the “kerrd” model. The mass of the black hole, distance to the source and inclination angle of the disk

were taken to be $12.4M_{\odot}$, 8.6 kpc and 60° (Reid et al. 2014) respectively. The colour factor was fixed to 1.7 (Shimura & Takahara 1995).

To take into account a relativistically smeared Iron fluorescence line, the model “kerrdisk” (Brenneman & Reynolds 2006) was used. While the “kerrd” model implicitly assumes a fast spinning black hole, the spin is a parameter for “kerrdisk” which was fixed at 0.98 (Blum et al. 2009), as the spectral fitting was found to be insensitive to its value. For the kerrdisk the emissivity index for both the inner and outer parts of the disk was fixed at 1.8 (Blum et al. 2009). The rest frame energy of the iron line was fixed at 6.4 keV (Blum et al. 2009). The inner radius was tied to that used for the “kerrd” after dividing by

an appropriate factor of 1.235, since for “kerrd”, the radius is measured in r_g , while for the kerrdisk it is in units of the radius of marginal stability. Absorption by intervening matter was modelled using “tbabs” (Wilms et al. 2000) with a column density fixed at $4 \times 10^{22} \text{cm}^{-2}$ (Blum et al. 2009). Representative spectra for a χ , intermediate and heartbeat state are shown in figure 2. Note that for the spectra of heartbeat state the iron line component is insignificant. Table 1 lists the best fit values of the parameters which are the accretion rate, inner disk radius, the fraction scattered into the Comptonizing medium, the index of the Comptonized spectrum and flux in the line emission.

3. RESULTS

The upper left panel of Figure 3 shows the variation of the QPO frequency with radius where a broad anti-correlation is visible, however, it is difficult to quantify the dependence because of the significant scatter. Indeed, the scatter suggests that the QPO frequency depends not only on the inner radius but also on some other parameter. The upper right and bottom panels of Figure 3 show the variation of the frequency with the accretion rate and the accretion rate with inner radii, where again there seems to be a correlation but with a large scatter. However, if one considers the frequency to depend both on the radius and the accretion rate and in particular if it is of the form $\propto \dot{M}F(R_{in})$ then the correlation is significantly better. This is illustrated in left panel of Figure 4 where the QPO frequency divided by the accretion rate is plotted against the inner radius. More pertinently the variation is the same as predicted by the standard accretion model for the dynamic frequency (Equation 3) represented by lines for different values of the spin parameter a . Note that the predicted functional form depends only on a and the normalization factor N which should be of order unity. While a formal fit gives $a = 0.973 \pm 0.002$, we also show the variation for two different values of $a = .91$ and $a = .99$ to illustrate the constraints the data imposes on a .

It is interesting to note that the best fit value of the black hole spin parameter obtained here is $a \sim 0.973 \pm 0.002$ which is consistent with $a = 0.98 \pm 0.01$ obtained independently by fitting the relativistically blurred reflection model to the broad band spectrum from Suzaku (Blum et al. 2009). While earlier results using RXTE and ASCA spectra gave contradictory results (McClintock et al. 2006; Middleton et al. 2006), the better spectral resolution of Suzaku and broad band analysis makes the results obtained by Blum et al. (2009) more reliable. We stress that the consistent determination of the spin parameter using two completely independent different methods, significantly strengthens the interpretation present in this work.

We emphasize that primary result used in this work, i.e. the estimate of the inner disk radii is not sensitive to the relativistic “kerrd” and “kerrdisk” models and they have been invoked for consistency. An alternate empirical model “tbabs*(simpl*diskbb+Gaussian)” provides nearly the same estimates of the inner radii as shown in right panel of Figure 4 where the two radii estimates are compared. There are two primary reasons for obtaining a reliable value of the radii which are (a) the

presence of low energy data from SXT and (b) the use of “simpl” to model the Comptonization instead of a power-law. This is illustrated in right panel of Figure 4, where the radii estimates without the SXT data (using the same empirical model (“tbabs*(simpl*diskbb+Gaussian)”) is plotted against that obtained from the relativistic models with SXT. Without SXT data the radii estimated are systematically lower and not correlated with the ones obtained when SXT data is considered. The right panel of Figure 4 also shows the case, when a power-law model is used instead of “simpl” (with SXT data). In this case also the radii obtained is systematically under estimated and not well correlated with the values estimated when “simpl” is used.

During the heartbeat state, the overall flux and spectra evolves (Rawat et al. 2019), while here we have considered a time-averaged spectrum. To verify the impact of this on the results presented, we performed flux resolved spectroscopy for all heartbeat observations by dividing the data into three flux levels and obtaining the corresponding spectra. We find that the qualitative nature as shown by the left panel of Figure 4 does not change with best fit values, $a = 0.968 \pm 0.002$ and $N = 0.24 \pm 0.01$ with reduced $\chi^2 \sim 1.1$, close to the ones obtained using time-averaged spectra.

4. DISCUSSION AND SUMMARY

The result obtained in this paper relies on the accuracy of some measured and theoretically estimated quantities. Future improvement on the estimate of these would refine the fitting presented here and can provide a robust value of the spin parameter. These include the uncertainties in (a) the estimated distance to the source, mass of the black hole and the inclination angle used; (b) the effective area and response of the LAXPC and SXT detectors, and (c) the theoretically estimated colour factor, especially since this was done for a non-spinning black hole (Shimura & Takahara 1995). Note that most of these uncertainties are independent of each other and will give rise to a secular shift in the radii and accretion rate.

The analysis has been done by fixing the neutral column density value, nH at $4 \times 10^{22} \text{cm}^{-2}$ as obtained by Blum et al 2009 using Suzaku data. If we instead allow it to vary its value ranges from $3.5 \times 10^{22} \text{cm}^{-2}$ to $4 \times 10^{22} \text{cm}^{-2}$ for different orbits with a typical error of $0.1 \times 10^{22} \text{cm}^{-2}$. Since we expect the column density not to vary during the course of the observation we have used the value obtained by Blum et al. (2009). If instead we use the average value obtained from the present observation, i.e. we fix it to $3.75 \times 10^{22} \text{cm}^{-2}$, we get qualitatively similar results, with the best fit values for the spin parameter and normalization to be $a = 0.986 \pm 0.002$ and $N = 0.18 \pm 0.01$.

It is interesting to note that for small values of radius (i.e. $r \sim 4r_g$) the radial functional form of Equation 3, is approximately $1/r$ instead of $1/r^{2.5}$ due to its dependence on the relativistic terms, A,B,D,E and L. This means that the QPO frequency is roughly proportional to \dot{M}/R_{in} , which in turn is proportional to the disk flux. Thus, an approximate dependence of the QPO frequency on total flux (if the disk component dominates) is expected in this scenario. Moreover, the spectral index of the Comptonization component may also depends on

Table 1
Spectral Parameters for GRS 1915+105 in 1.0-50.0 keV energy range

Exposure time (sec)	State	QPO frequency (Hz)	Accretion rate $10^{18} \text{ gm s}^{-1}$	Inner radius (R_g)	Fraction scatter	Gamma	Flux in line emission $10^{-2} \text{ photons cm}^{-2} \text{ s}^{-1}$	χ^2/Dof
<i>28th March 2017</i>								
1199	χ class	$3.59^{+0.01}_{-0.01}$	$0.67^{+0.01}_{-0.02}$	$4.62^{+0.15}_{-0.06}$	$0.42^{+0.01}_{-0.01}$	$2.169^{+0.005}_{-0.005}$	$1.1^{+0.2}_{-0.1}$	488.7/426
1199	χ class	$3.46^{+0.02}_{-0.02}$	$0.74^{+0.04}_{-0.03}$	$5.25^{+0.27}_{-0.24}$	$0.43^{+0.02}_{-0.02}$	$2.169^{+0.011}_{-0.005}$	$1.1^{+0.2}_{-0.2}$	492.1/424
1203	χ class	$3.65^{+0.01}_{-0.02}$	$0.77^{+0.03}_{-0.03}$	$5.31^{+0.19}_{-0.15}$	$0.45^{+0.02}_{-0.01}$	$2.221^{+0.006}_{-0.007}$	$1.0^{+0.2}_{-0.2}$	509.4/431
903	<i>IMS</i>	$4.08^{+0.03}_{-0.02}$	$0.71^{+0.03}_{-0.04}$	$4.20^{+0.20}_{-0.29}$	$0.39^{+0.01}_{-0.01}$	$2.223^{+0.009}_{-0.011}$	$0.9^{+0.3}_{-0.2}$	489.4/411
477	<i>IMS</i>	$4.17^{+0.03}_{-0.03}$	$0.74^{+0.04}_{-0.04}$	$4.53^{+0.25}_{-0.30}$	$0.40^{+0.02}_{-0.01}$	$2.247^{+0.012}_{-0.013}$	$0.9^{+0.3}_{-0.3}$	298.8/322
840	<i>IMS</i>	$4.38^{+0.07}_{-0.06}$	$0.68^{+0.02}_{-0.04}$	$3.58^{+0.17}_{-0.27}$	$0.35^{+0.01}_{-0.01}$	$2.260^{+0.013}_{-0.014}$	—	419.1/410
1209	<i>HS</i>	$5.08^{+0.03}_{-0.03}$	$0.65^{+0.01}_{-0.03}$	$3.02^{+0.09}_{-0.24}$	$0.29^{+0.01}_{-0.01}$	$2.255^{+0.014}_{-0.017}$	—	519.6/437
1211	<i>HS</i>	$5.15^{+0.03}_{-0.03}$	$0.64^{+0.03}_{-0.00}$	$2.90^{+0.18}_{-0.03}$	$0.29^{+0.01}_{-0.01}$	$2.241^{+0.014}_{-0.009}$	—	492.7/436
1213	<i>HS</i>	$5.33^{+0.03}_{-0.03}$	$0.66^{+0.02}_{-0.02}$	$2.80^{+0.12}_{-0.09}$	$0.27^{+0.01}_{-0.01}$	$2.239^{+0.012}_{-0.006}$	—	539.4/439
1216	<i>HS</i>	$5.42^{+0.03}_{-0.03}$	$0.69^{+0.01}_{-0.01}$	$3.03^{+0.09}_{-0.14}$	$0.26^{+0.01}_{-0.01}$	$2.252^{+0.012}_{-0.007}$	—	490.5/437
<i>1st April 2017</i>								
634	χ class	$4.05^{+0.02}_{-0.02}$	$0.78^{+0.04}_{-0.04}$	$4.84^{+0.32}_{-0.31}$	$0.38^{+0.01}_{-0.01}$	$2.219^{+0.012}_{-0.012}$	$1.0^{+0.2}_{-0.2}$	347.2/374
204	χ class	$4.67^{+0.04}_{-0.04}$	$0.79^{+0.06}_{-0.07}$	$4.42^{+0.35}_{-0.47}$	$0.36^{+0.01}_{-0.01}$	$2.274^{+0.017}_{-0.020}$	$0.7^{+0.4}_{-0.2}$	222.3/199
748	<i>HS</i>	$5.13^{+0.03}_{-0.04}$	$0.72^{+0.02}_{-0.02}$	$3.44^{+0.12}_{-0.20}$	$0.31^{+0.00}_{-0.00}$	$2.278^{+0.014}_{-0.003}$	—	438.1/407
1175	<i>HS</i>	$5.13^{+0.02}_{-0.02}$	$0.71^{+0.02}_{-0.03}$	$3.27^{+0.13}_{-0.17}$	$0.31^{+0.01}_{-0.01}$	$2.287^{+0.015}_{-0.014}$	—	519.5/439
1260	<i>HS</i>	$5.12^{+0.01}_{-0.01}$	$0.72^{+0.02}_{-0.02}$	$3.44^{+0.14}_{-0.13}$	$0.30^{+0.01}_{-0.01}$	$2.262^{+0.013}_{-0.013}$	—	458.9/439
762	<i>HS</i>	$5.27^{+0.04}_{-0.04}$	$0.69^{+0.04}_{-0.01}$	$3.09^{+0.22}_{-0.10}$	$0.28^{+0.01}_{-0.01}$	$2.245^{+0.014}_{-0.014}$	—	459.4/411

Note. — Here, IMS and HS stand for intermediate and Heartbeat states respectively.

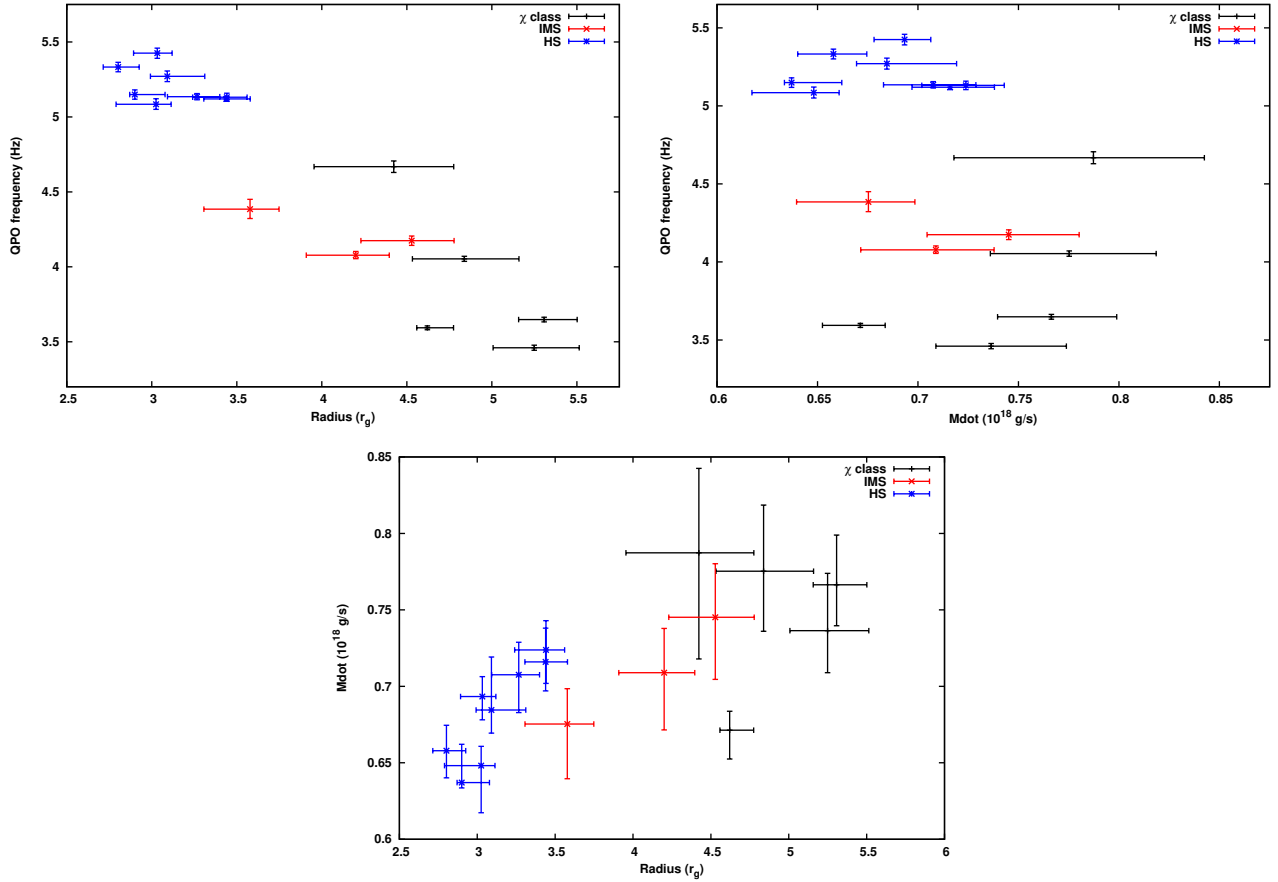


Figure 3. The variation of QPO frequencies with inner disk radii and Accretion rate are shown in upper left and upper right panels respectively. The bottom panel shows the variation of the accretion rate with inner disk radii.

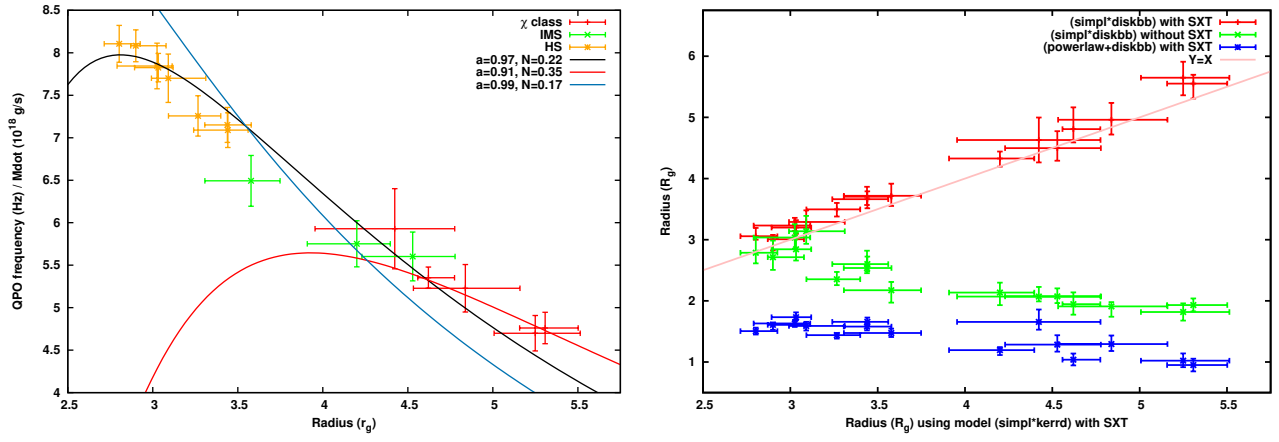


Figure 4. Left panel shows variation of QPO frequency divided by the accretion rate with inner disk radii. The lines represent the $\frac{f_{dyn}}{M_{18}}$ as predicted by the relativistic standard accretion disk model (Equation 3) for dimensionless spin parameter $a = 0.973 \pm 0.002$ (best fit with $N = 0.22 \pm 0.01$ and reduced $\chi^2 \sim 0.5$), $a = 0.91$ ($N = 0.35$) and $a = 0.99$ ($N = 0.17$). In the right panel we show a comparison of the estimated values of the inner disk radii.

the disk flux, leading to a QPO frequency dependence on the index. For the spectral fitting results presented here, there is indeed a dependence of the spectral index on the disk flux, which will be physically interpreted in a later work where the evolution of the spectral parameters will be described in more detail. Here, we note, that in this interpretation dependence of QPO frequency on spectral index (Bhargava et al. 2019) is an indirect consequence of it being the dynamical frequency of a truncated disk as explicitly mentioned in Titarchuk & Osherovich (1999).

Since the QPO frequency depends both on the radius and accretion rate, this favours models based on hydrodynamics, especially for example the coronal oscillatory one (Titarchuk & Osherovich 1999; Titarchuk & Fiorito 2004; Shaposhnikov & Titarchuk 2007) where the frequency is indeed identified with the dynamic one. However, other models such as the Accretion-Ejection Instability (Varnière et al. 2002; Tagger & Pellat 1999) are also promising, since evidence is provided for a driving instability. Although some of these theoretical models have different identification of the QPO frequency, the result presented here provides now a strong foothold, on which sophisticated models can be developed.

In summary, we exploit the broad band capability of *AstroSat* to study the spectral properties of GRS 1915+105 with the QPO frequency. We find that the frequency depends on the accretion rate and inner radius of the disk, just as it was predicted for the dynamical frequency of a relativistic accretion disk. Thus, we identify the QPO frequency as the inverse of the sound cross time from the inner disk radius where strong General Relativistic effects dominate.

5. ACKNOWLEDGMENT

We thank the referee for constructive comments. This research has used the data of *AstroSat* mission of the Indian Space Research Organisation (ISRO), archived at the Indian Space Science Data Centre. The authors would like to acknowledge the support from the LAXPC Payload Operation Center (POC) and SXT POC at the TIFR, Mumbai for providing support in data reduction.

REFERENCES

- Agrawal, P. C. 2017, *Journal of Astrophysics and Astronomy*, 38, 27, doi: 10.1007/s12036-017-9449-6
- Agrawal, P. C., Yadav, J. S., Antia, H. M., et al. 2017, *Journal of Astrophysics and Astronomy*, 38, 30, doi: 10.1007/s12036-017-9451-z
- Arnaud, K. A. 1996, in *Astronomical Society of the Pacific Conference Series*, Vol. 101, *Astronomical Data Analysis Software and Systems V*, ed. G. H. Jacoby & J. Barnes, 17
- Belloni, T., Psaltis, D., & van der Klis, M. 2002, *ApJ*, 572, 392, doi: 10.1086/340290
- Bhargava, Y., Belloni, T., Bhattacharya, D., & Misra, R. 2019, *MNRAS*, 488, 720, doi: 10.1093/mnras/stz1774
- Blum, J. L., Miller, J. M., Fabian, A. C., et al. 2009, *ApJ*, 706, 60, doi: 10.1088/0004-637X/706/1/60
- Brenneman, L. W., & Reynolds, C. S. 2006, *ApJ*, 652, 1028, doi: 10.1086/508146
- Casella, P., Belloni, T., Homan, J., & Stella, L. 2004, *A&A*, 426, 587, doi: 10.1051/0004-6361:20041231
- Ebisawa, K., Życki, P., Kubota, A., Mizuno, T., & Watarai, K.-y. 2003, *ApJ*, 597, 780, doi: 10.1086/378586
- Homan, J., Wijnands, R., van der Klis, M., et al. 2001, *ApJS*, 132, 377, doi: 10.1086/318954
- McClintock, J. E., Shafee, R., Narayan, R., et al. 2006, *ApJ*, 652, 518, doi: 10.1086/508457
- Middleton, M., Done, C., Gierliński, M., & Davis, S. W. 2006, *MNRAS*, 373, 1004, doi: 10.1111/j.1365-2966.2006.11077.x
- Mikles, V. J., Varniere, P., Eikenberry, S. S., Rodriguez, J., & Rothstein, D. 2009, *ApJL*, 694, L132, doi: 10.1088/0004-637X/694/2/L132
- Motta, S. E., Belloni, T. M., Stella, L., Muñoz-Darias, T., & Fender, R. 2014, *MNRAS*, 437, 2554, doi: 10.1093/mnras/stt2068
- Muno, M. P., Morgan, E. H., & Remillard, R. A. 1999, *ApJ*, 527, 321, doi: 10.1086/308063
- Narayan, R., & McClintock, J. E. 2008, *New A Rev.*, 51, 733, doi: 10.1016/j.newar.2008.03.002
- Novikov, I. D., & Thorne, K. S. 1973, in *Black Holes (Les Astres Occlus)*, 343–450
- Psaltis, D., Belloni, T., & van der Klis, M. 1999, *ApJ*, 520, 262, doi: 10.1086/307436
- Rawat, D., Pahari, M., Yadav, J. S., et al. 2019, *ApJ*, 870, 4, doi: 10.3847/1538-4357/aafed
- Reid, M. J., McClintock, J. E., Steiner, J. F., et al. 2014, *ApJ*, 796, 2, doi: 10.1088/0004-637X/796/1/2
- Remillard, R. A., Sobczak, G. J., Muno, M. P., & McClintock, J. E. 2002, *ApJ*, 564, 962, doi: 10.1086/324276
- Shakura, N. I., & Sunyaev, R. A. 1973, *A&A*, 500, 33
- Shapiro, S. L., Lightman, A. P., & Eardley, D. M. 1976, *ApJ*, 204, 187, doi: 10.1086/154162
- Shaposhnikov, N., & Titarchuk, L. 2007, *ApJ*, 663, 445, doi: 10.1086/518110
- Shimura, T., & Takahara, F. 1995, *ApJ*, 445, 780, doi: 10.1086/175740
- Singh, K. P., Stewart, G. C., Chandra, S., et al. 2016, in *Society of Photo-Optical Instrumentation Engineers (SPIE) Conference Series*, Vol. 9905, *Proc. SPIE*, 99051E
- Singh, K. P., Stewart, G. C., Westergaard, N. J., et al. 2017, *Journal of Astrophysics and Astronomy*, 38, 29, doi: 10.1007/s12036-017-9448-7
- Sobczak, G. J., McClintock, J. E., Remillard, R. A., et al. 2000, *ApJ*, 531, 537, doi: 10.1086/308463
- Steiner, J. F., Narayan, R., McClintock, J. E., & Ebisawa, K. 2009, *PASP*, 121, 1279, doi: 10.1086/648535
- Stella, L., Vietri, M., & Morsink, S. 1999a, *Astrophysical Letters and Communications*, 38, 57
- Stella, L., Vietri, M., & Morsink, S. M. 1999b, *ApJL*, 524, L63, doi: 10.1086/312291
- Tagger, M., & Pellat, R. 1999, *A&A*, 349, 1003, <https://arxiv.org/abs/astro-ph/9907267>
- Titarchuk, L., & Fiorito, R. 2004, *ApJ*, 612, 988, doi: 10.1086/422573
- Titarchuk, L., & Osherovich, V. 1999, *ApJL*, 518, L95, doi: 10.1086/312083
- van der Klis, M. 2005, *Astronomische Nachrichten*, 326, 798, doi: 10.1002/asna.200510416
- Varnière, P., Rodriguez, J., & Tagger, M. 2002, *A&A*, 387, 497, doi: 10.1051/0004-6361:20020401
- Wijnands, R., Homan, J., & van der Klis, M. 1999, *ApJL*, 526, L33, doi: 10.1086/312365
- Wilms, J., Allen, A., & McCray, R. 2000, *ApJ*, 542, 914, doi: 10.1086/317016
- Yadav, J. S., Agrawal, P. C., Antia, H. M., et al. 2016, in *Society of Photo-Optical Instrumentation Engineers (SPIE) Conference Series*, Vol. 9905, *Proc. SPIE*, 99051D